



2 Can thin cirrus clouds in the tropics provide a 3 solution to the faint young Sun paradox?

4 Roberto Rondanelli^{1,2} and Richard S. Lindzen¹

5 Received 13 March 2009; revised 8 September 2009; accepted 22 September 2009; published XX Month 2010.

6 [1] In this paper we present radiative-convective simulations to test the idea that tropical
7 cirrus clouds, acting as a negative feedback on climate, can provide a solution to the faint
8 young Sun paradox. We find that global mean surface temperatures above freezing can
9 indeed be found for luminosities larger than about 0.8 (corresponding to ~ 2.9 Ga and
10 nearly complete tropical cirrus coverage). For luminosities smaller than 0.8, even though
11 global mean surface temperatures are below freezing, tropical mean temperatures are still
12 above freezing, indicating the possibility of a partially ice-free Earth for the Early
13 Archean. We discuss possible mechanisms for the functioning of this negative feedback.
14 While it is feasible for tropical cirrus to completely eliminate the paradox, it is similarly
15 possible for tropical cirrus to reduce the amounts of other greenhouse gases needed
16 for solving the paradox and therefore easing the constraints on CO_2 and CH_4 that appear to
17 be in disagreement with geological evidence.

18 **Citation:** Rondanelli, R., and R. S. Lindzen (2010), Can thin cirrus clouds in the tropics provide a solution to the faint young Sun
19 paradox?, *J. Geophys. Res.*, 115, XXXXXX, doi:10.1029/2009JD012050.

21 1. Introduction

22 [2] Models for the evolution of the Sun during the main
23 sequence call for a reduced solar luminosity and therefore a
24 reduced Earth's solar constant of about $S = 0.75 S_0$ around
25 3.8 Ga (with S_0 the present solar constant $\sim 1353 \text{ W/m}^2$)
26 [Schwarzschild, 1958; Newman and Rood, 1977]. At the same
27 time, geological evidence shows the presence of a
28 stable ocean and liquid water in the planet at least after
29 3.9 Ga (and perhaps even earlier [e.g., Wilde *et al.*, 2001;
30 Pinti, 2005]). The fact that simple models of the Earth's
31 climate cannot reconcile the reduced luminosity with the
32 presence of liquid water (and the absence of glacial deposits)
33 has become known as the faint young Sun paradox [Sagan
34 and Mullen, 1972]. The paradox hinges on the assumption
35 of a constant atmospheric composition or, more precisely,
36 on the assumption of a constant atmospheric greenhouse
37 effect and a constant atmospheric solar reflectivity (both
38 including gases and clouds). Just for illustration purposes,
39 one can use a crude zero-dimensional energy balance for the
40 atmosphere to calculate the mean global surface temperature
41 (T_s) [e.g., Catling and Kasting, 2007],

$$22 \quad T_s = T_g + \left(\frac{(1-A)S}{4\sigma} \right)^{\frac{1}{4}}, \quad (1)$$

43 where A is the planetary albedo and T_g is a temperature that
44 encapsulates the greenhouse effect of the atmosphere and

clouds. For current climate with $A = 0.3$ and $T_g = 34$, $T_s = 45$
288 K. According to the standard solar model, the 46
luminosity, and therefore the variation of the solar constant 47
can be approximated by [Gough, 1981] 48

$$S = \frac{S_0}{1 + 0.4t/4.6}, \quad (2)$$

where t is the time in Ga. 50

[3] Under the assumption of a constant greenhouse effect, 51
the simple zero-dimensional model gives $T_s = 269 \text{ K}$ for a 52
solar luminosity of $S = 0.75 S_0$, ~ 3.9 Ga. T_s rises above 53
freezing for $S \sim 0.79 S_0$, which corresponds to 2.9 Ga. It 54
might seem that a much reduced value of A in equation (1) 55
could increase the temperature above freezing. However, 56
the absence of clouds (the main driver of the albedo) would 57
also result in a significant reduction of the greenhouse 58
effect. A first correction to the simple model is to include 59
a water vapor feedback by assuming a constant relative 60
humidity (instead of the implicit assumption of constant 61
specific humidity). By including this positive water vapor 62
feedback in a 1-D radiative convective model one increases 63
the time range of the paradox: a colder surface temperature 64
implies a drier atmosphere and a reduced greenhouse effect. 65
For instance, Kasting *et al.* [1988] found that T_s remains 66
below freezing up until ~ 2 Ga or $S \sim 0.85 S_0$. Moreover, 67
Pierrehumbert [2010] shows that including an ice-albedo 68
feedback the paradox is even more dramatic and the 69
solution for $S = 0.75 S_0$ is a snowball Earth with $T_s = 70$
228 K (however, see Cogley and Henderson-Sellers [1984] 71
for arguments on a much reduced role for the ice-albedo 72
feedback on the early Earth). 73

[4] Sagan and Mullen [1972] first pointed out the exis- 74
tence of the paradox and suggested that trace amounts of 75

¹Department of Earth, Atmospheric and Planetary Sciences, Massachusetts Institute of Technology, Cambridge, Massachusetts, USA.

²Department of Geophysics, University of Chile, Santiago, Chile.

76 NH₃ could solve the paradox. This solution was later found
 77 untenable due to the relatively small lifetime of NH₃ to
 78 photolysis in an anoxic atmosphere [Kuhn and Atreya,
 79 1979]. Most of the solutions to the paradox have relied on
 80 changes in T_g produced by either CO₂, CH₄ or both [e.g.,
 81 Hart, 1978; Owen et al., 1979; Kasting, 1987; Kasting et
 82 al., 1988; Pavlov et al., 2000; Haqq-Misra et al., 2008].
 83 Solutions that involve high CO₂ atmospheric concentrations
 84 are particularly appealing given the existence of large
 85 reservoirs of carbon in the Earth's mantle and continents
 86 (and the relative smallness of the atmospheric and oceanic
 87 reservoirs). The temperature dependence of the silicate
 88 weathering rate (mainly through the temperature dependence
 89 of the precipitation) can act as a negative feedback on climate
 90 acting through the CO₂ geological cycle [Walker et al., 1981].
 91 According to this mechanism, climates colder than present
 92 are expected to have a higher CO₂ concentrations, compen-
 93 sating to some extent for the reduced solar luminosity.

94 [5] However, some geological evidence from paleosols
 95 and other proxies indicates that CO₂ concentrations must be
 96 at least ten times smaller than those required to produce
 97 mean surface temperatures above freezing in 1-D radiative-
 98 convective models [Rye et al., 1995; Rollinson, 2007].
 99 Zahnle and Sleep [2002] also argue on the basis of theo-
 100 retical calculations of the carbon geological cycle, that high
 101 CO₂ concentrations are implausible. If the geological evi-
 102 dence is taken at face value, the paradox seems to be
 103 unresolved [Shaw, 2008]. This realization has prompted
 104 even the reconsideration of the relevance of the standard
 105 model for solar evolution and therefore the faintness of the
 106 early Sun [e.g., Sackmann and Boothroyd, 2003]. However,
 107 evidence for the standard solar model is strong. In particu-
 108 lar, solar analogs appear to show no evidence for the mag-
 109 nitude and time scale of mass loss required to explain
 110 an early bright Sun [Minton and Malhotra, 2007].

111 [6] The meridional heat transport can also change under
 112 different forcing conditions, potentially providing a stabi-
 113 lizing influence on climate, specially for the onset of
 114 snowball solutions [e.g., Lindzen and Farrell, 1980]. The
 115 moderating influence of meridional heat transport has been
 116 discussed in the context of the faint young Sun paradox by
 117 Endal and Schatten [1982], who proposed a much more
 118 effective ocean heat transport in an early Earth with small
 119 continents. However, a more effective heat transport would
 120 also produce a larger value for the critical insolation for the
 121 onset of a snowball Earth. Gerard et al. [1990], based on the
 122 maximum entropy principle [Paltridge, 1978], deduced that
 123 the heat transport becomes less efficient for lower solar
 124 luminosities and therefore they obtain solutions that are
 125 stable to an ice-albedo feedback for the whole evolution of
 126 the solar constant.

127 [7] Besides purely dynamical or radiative mechanisms to
 128 account for the moderate temperatures under lower solar
 129 luminosity, the rise of life and subsequent changes in
 130 atmospheric composition may have played a role in the
 131 climate stabilization required to explain the paradox. For
 132 instance, the rise of early bacteria could have increased
 133 methane fluxes into an early anoxic atmosphere [e.g.,
 134 Pavlov et al., 2000] providing methane concentrations of
 135 about 100 times present concentrations [Pavlov et al.,
 136 2003]. The enhancement of the weathering rate due to the
 137 rise of life has also been proposed as a negative feedback on

climate [Volk, 1987; Schwartzman and Volk, 1989, 2004] 138
 and moreover as a potential self-regulating mechanism for 139
 the biosphere [Lovelock and Whitfield, 1982]. 140

[8] Water clouds on the other hand, have been only rarely 141
 invoked as a possible solution to the paradox, although 142
 changes in their composition, height and areal extent can 143
 potentially provide large changes in both A and T_g . When 144
 studying the effect of greenhouse gases, clouds properties 145
 are usually kept constant. The rationale and limitations for 146
 the assumption of constant cloud properties are summarized 147
 by Kasting and Catling [2003]: "If the goal is to determine 148
 what is required to create a climate similar to that of today, it 149
 is reasonable to assume no change in cloud properties. For 150
 model planets that are either much hotter or much colder 151
 than present Earth, however, the neglect of cloud feedback 152
 may lead to serious error." The matter of how much colder 153
 (or hotter) a climate should be so that the effect of cloud 154
 feedbacks becomes important has been the subject of some 155
 previous studies on the role of clouds in the early Earth 156
 climate [Henderson-Sellers and Cogley, 1982; Rossow et 157
 al., 1982]. In those studies a decrease in cloud liquid water 158
 in colder climates is associated with a decrease in planetary 159
 albedo large enough to produce mean global surface tem- 160
 peratures above freezing for $S \gtrsim 0.8 S_0$. 161

[9] Here, we focus on testing the feasibility of a solution 162
 based on changes in the cirrus cloud coverage in the tropics. 163
 We are primarily interested whether a plausible change in 164
 the coverage of thin cirrus clouds can solve the faint young 165
 Sun paradox, regardless of the origin of such a change. We 166
 focus on tropical cirrus clouds because contrary to extra- 167
 tropical clouds, in which cloud coverage is mostly related to 168
 the relative area of ascent and descent in baroclinic dis- 169
 turbances, the mechanism of formation of cirrus in the 170
 tropics appears to be particularly susceptible to a surface 171
 temperature dependence. An example of a mechanism that 172
 could relate sea surface temperature to thin cirrus cloud 173
 coverage is the iris hypothesis proposed by Lindzen et al. 174
 [2001]. We defer to section 4 the discussion of this 175
 particular mechanism. 176

[10] Thin cirrus clouds are a ubiquitous feature of the 177
 current tropical atmosphere. Recent global data using sat- 178
 ellite lidar and radar instruments place the frequency of thin 179
 cirrus clouds ($\tau < 3-4$) at $\sim 25\%$ over the tropics ($30^\circ\text{S}-$ 180
 30°N) [Sassen et al., 2008]. Trajectory studies show that at 181
 least two mechanisms explain the formation of cirrus clouds 182
 in the tropics; a direct detrainment from convective clouds 183
 and also a triggering by gravity waves further away from the 184
 original convective region [Mace et al., 2006]. Although 185
 cirrus clouds are believed to have a net positive radiative 186
 effect, there remains uncertainty on this point [Liou, 2005]. 187
 Nevertheless, recent satellite estimations of the cloud radi- 188
 ative effect of cirrus clouds [Choi and Ho, 2006] seem to 189
 confirm the long-held idea that thin cirrus clouds (that is 190
 clouds with visible optical depths $\tau \lesssim 10$) have a much 191
 larger infrared heating effect than a shortwave cooling, and 192
 therefore a strong positive cloud radiative effect. 193

[11] One-dimensional radiative convective simulations, 194
 including at least some representation of cirrus clouds, have 195
 already shown the potential of thin cirrus clouds to produce 196
 significant surface warming. In the seminal paper by Manabe 197
 and Wetherald [1967], the addition of a layer of full black 198
 cirrus cloud was enough to increase the equilibrium surface 199

200 temperature from 280 K to 320 K. Similarly, *Liou and*
 201 *Gebhart* [1982] show radiative-convective equilibrium sim- 258
 202 ulations in which the inclusion of a thin cirrus cloud can 259
 203 increase surface temperatures to ~ 320 K for total coverage, 260
 204 with the surface temperature being relatively independent of 261
 205 the height of the cloud base. In the next sections, we present 262
 206 results from a simple radiative-convective model in which 263
 207 the tropical thin cirrus cloud coverage (f) is specified. 264

208 2. Model Assumptions

209 [12] The 1-D model is a simple radiative-convective 265
 210 equilibrium model based on the original formulation by 266
 211 *Manabe and Strickler* [1964] and *Manabe and Wetherald* 267
 212 [1967]. The model has 140 levels in pressure from 1000 hPa 268
 213 to 0.04 hPa, following the sigma-level pressure coordinates 269
 214 defined by *Manabe and Wetherald* [1967]. The model is run 270
 215 for 600 days from an initial moist adiabatic atmosphere with 271
 216 surface temperature of 300 K, with time step of 1 day 272
 217 (equilibrium between incoming shortwave and outgoing 273
 218 longwave radiation is reached within less than 1 W/m^2). 274
 219 We use a similar relative humidity profile as in *Manabe and* 275
 220 *Wetherald* [1967] with a surface relative humidity of 0.8 and 276
 221 a constant stratospheric water vapor mixing ratio of $3 \times$ 277
 222 10^{-6} . At each time step we use solar and infrared radiative 278
 223 parameterizations (developed for general circulation models 279
 224 [*Chou and Suarez*, 2002; *Chou et al.*, 2003]) to estimate the 280
 225 radiative heating rates in each vertical layer. A convective 281
 226 adjustment is performed at each time step, so unstable layers 282
 227 are adjusted to a reversible moist adiabat (which at least for 283
 228 the tropics seems to be a very good approximation for the 284
 229 temperature vertical distribution [*Emanuel*, 2007]). In all the 285
 230 runs, unless otherwise noted, the concentration of the 286
 231 radiatively active gases (except for water vapor) is kept 287
 232 fixed and approximately equal to the present atmospheric 288
 233 levels (PAL). That is, $\text{CO}_2 = 350$ ppmv and $\text{CH}_4 = 1.75$ ppmv. 289

234 [13] We assess the effect of the coverage of tropical cirrus 290
 235 clouds on surface temperature with some very simple 291
 236 assumptions. The effect of clouds other than thin cirrus 292
 237 (hereafter $\tau < 9$) is not explicitly incorporated, but rather 293
 238 enters as a constant planetary albedo fixed to about 0.2 (this 294
 239 is only part of the planetary albedo, since the radiative 295
 240 parameterization calculates explicitly the scattering by the 296
 241 clear atmosphere and thin cirrus clouds). In this way an 297
 242 incoming solar radiation and a coverage of 0.16 for thin 298
 243 cirrus, will provide a surface temperature close to the 299
 244 observed in the present (298 K for the mean tropical 300
 245 temperature). The incoming solar radiation that provides 301
 246 the current tropical average temperature ($\sim 285 \text{ W/m}^2$ after 302
 247 correcting by the solar zenith angle and constant planetary 303
 248 albedo), will serve as a basis for changing the solar constant 304
 249 in the model, mimicking the solar history. The solar zenith 305
 250 angle is kept constant and equal to 60° . The treatment of 306
 251 clouds in the radiative parameterization is explained in 307
 252 detail by *Chou and Suarez* [2002]; *Chou et al.* [2003]. 308
 253 The cloud optical thickness in the visible spectral region 309
 254 (τ_c) is a function of both the effective radius of the cloud 310
 255 particles r_e and the ice water path (IWP) of the cloud, and it 311
 256 is parameterized as 312

$$\tau_c = \text{IWP} \frac{1.64}{r_e}, \quad (3)$$

where IWP has units of g m^{-2} and r_e has units of μm . The 258
 parameterization of the cloud radiative effect in the visible 259
 is independent of the solar spectral bands. The value of r_e is 260
 calculated according to the empirical regression by 261
McFarquhar [2001] as a function of both the local 262
 temperature and the value of the cloud water content. The 263
 parameterization of the infrared optical depth of the cloud, 264
 takes into account the absorption and scattering of radiation 265
 by the cloud [*Chou et al.*, 1999]. The extinction coefficient, 266
 the single scattering albedo and the asymmetry factor are all 267
 dependent on r_e and on the particular spectral band [*Chou et* 268
al., 2003]. By specifying the thickness of the cloud (here 269
 equal to one model vertical layer) and by specifying the 270
 cloud water content, both IWP and r_e can be calculated. 271

[14] In the control case, we specify the value of cloud 272
 liquid water content to $7 \times 10^{-4} \text{ g/g}$, so that a cloud with a 273
 thickness of 9 hPa results in an IWP $\sim 44 \text{ g/m}^2$. The cloud 274
 is first located at a fixed level of 200 hPa (we will discuss 275
 the effect of relaxing this assumption to make it consistent 276
 with the changes in the vertical temperature structure over 277
 the range of solar forcings). We use a single cloud as a 278
 proxy for the radiative effect of all types of thin cirrus 279
 clouds in the tropics. The selection of this particular cloud is 280
 not arbitrary, rather it is such that it roughly matches the 281
 radiative forcing from observations in current climate as 282
 estimated by *Choi and Ho* [2006]. For the control run, the 283
 selected cloud provides a longwave cloud radiative effect of 284
 $+115 \text{ W/m}^2$ and a shortwave cloud radiative effect of 285
 -50 W/m^2 . These values coincide roughly with the observed 286
 values derived by *Choi and Ho* [2006] for both the long- 287
 wave and the shortwave radiative effect as well as the net 288
 positive cloud radiative effect of these clouds, which is 289
 about $+46 \text{ W/m}^2$ for all clouds with $\tau < 4$. 290

291 3. Results

292 3.1. Single Column Radiative-Convective Simulation

[15] In the first run we explore the behavior of the tropical 293
 surface temperature in radiative convective equilibrium for 294
 different values of the thin cirrus cloud coverage. Figure 1a 295
 shows the results for this tropics-only column. For the 296
 current solar insolation S_0 and current cloud coverage $f \sim$ 297
 0.16 the surface temperature is ~ 298 K. An increase in the 298
 coverage of this thin cirrus cloud from $f = 0.16$ to $f = 1$ 299
 would produce an increase in the surface temperature in the 300
 tropics to about 325 K. From Figure 1a, we notice that the 301
 mean tropical temperature is above freezing for constant 302
 atmospheric conditions (lower gray line), even at solar 303
 insolutions of about $S \sim 0.81 S_0$. We note that the usual 304
 statement of the faint young Sun paradox is made in terms 305
 of mean surface temperature. Therefore a solution is con- 306
 sidered as such when the mean surface temperature is above 307
 freezing (hereafter, this is what we will consider a solution). 308
 A weaker version of the paradox can be envisioned in which 309
 temperatures are above freezing for a significantly large area 310
 of the planet. One can also envision a stronger version of the 311
 paradox in which one takes the absence of evidence of 312
 glaciation as an indication of a completely ice-free Earth. 313

[16] The three black dashed lines in Figures 1a–1d 314
 represent three different relative rates of change for the thin 315
 cirrus cloud coverage (so a $-10\%/K$ rate of change repre- 316
 sents a change from 0.16 to 0.176 from 298 K to 297 K. We 317

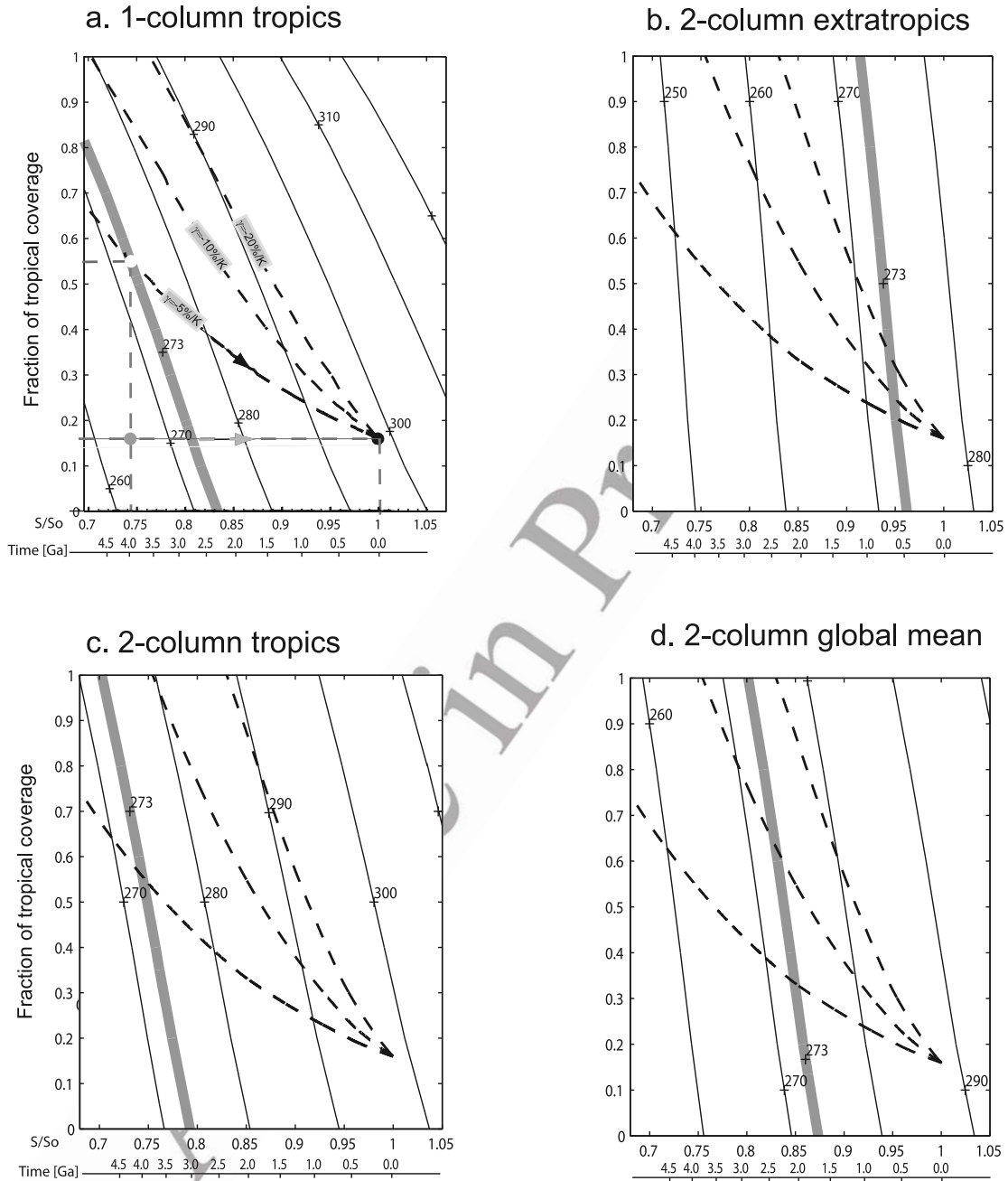


Figure 1. Equilibrium surface temperature corresponding to (a) one-column, tropics-only simulation, (b) extratropical column in the two-column simulation, (c) tropical column in the two-column simulation, and (d) global mean in the two-column simulation. The temperature is indicated by the solid black lines. In Figure 1a a black dot indicates current climate conditions. The white dot indicates the climate surface temperature corresponding to a luminosity of $\sim 0.74S_0$ and a cloud coverage of 0.55. This climate occurs for a rate of change of $-5\%/K$ in the coverage of thin cirrus clouds in the tropics. The two other dashed lines represent rates of change in the cloud coverage of $-10\%/K$ and $-20\%/K$ as labeled. The grey dot is the equilibrium temperature of a climate with the same luminosity as the white dot but with no cloud feedback. The time scale in the abscissa is calculated according to equation (2).

318 will denote this rate of change as $\gamma = \frac{1}{f} \frac{\partial f}{\partial T_t}$, where T_t is the
 319 mean tropical rate. The rate of change γ represents implicitly the magnitude of the climate feedback associated with
 320 increase in thin cirrus clouds. The dashed lines in each of
 321 the panels of Figure 1 are for magnitudes of $\gamma = -5\%/K$,
 322 $-10\%/K$ and $-20\%/K$. For this tropics-only case, to sustain
 323 surface temperatures above freezing for $S = 0.7 S_0$, one
 324

would need a cirrus coverage of about 0.8. This surface 325
 coverage is accomplished with a mere $-6\%/K$ change in the 326
 cloud coverage. 327

3.2. Two-Column Radiative-Convective Simulation 328

[17] Since in the previous simulation we only deal with a 329
 tropical column, we cannot test the paradox in its more 330

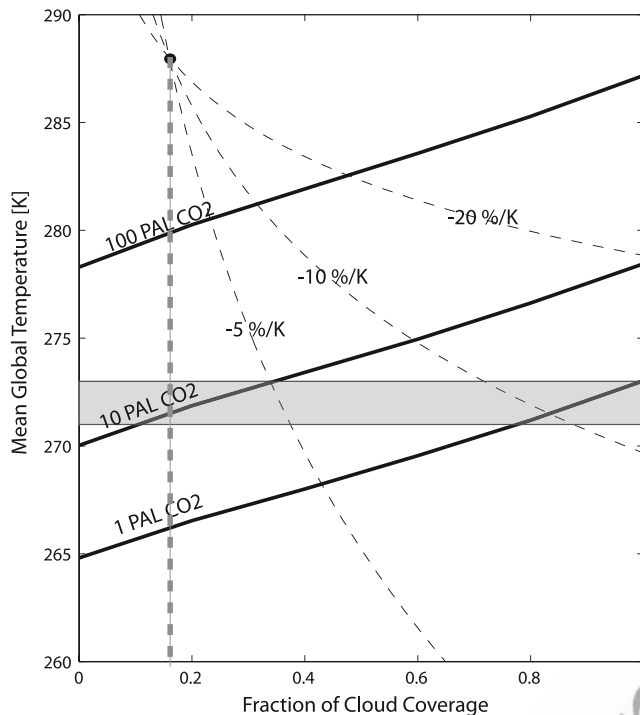


Figure 2. Mean surface temperature corresponding to the two-column radiative convective model for $S = 0.8S_0$. The black solid lines are three different concentrations of CO_2 (PAL stands for present atmospheric level). The dashed lines represent different rates of change in the thin cirrus cloud coverage from the present value of 0.16. The gray horizontal strip is meant to represent a range of temperatures for freezing water between 271 and 273 K.

331 usual framing, that is, with respect to global mean temper-
 332 ature. Also, since the incoming solar radiation in the single
 333 column has been tuned so as to produce the observed
 334 current tropical temperature, the heat transported out of
 335 the tropical column (implicit in the tuning) decreases in
 336 the same proportion as the solar insolation.

337 [18] We add an extratropical column to the model and we
 338 will assume a diffusive heat transport between the two
 339 columns, with a constant transport coefficient $K = 3 \times$
 340 $10^6 \text{ m}^2/\text{s}$ over the depth of the model, so that at each time
 341 step, the temperature in each layer is calculated as the sum
 342 of three tendencies; the radiative heating, the convective
 343 adjustment and the meridional transport between the
 344 columns.

345 [19] The results for the two-column simulations are
 346 shown in Figures 1b, 1c and 1d. Figure 1c can be directly
 347 compared to Figure 1a. We see that assumption of a
 348 diffusive transport makes the two-column tropics warmer
 349 than the single-column tropics for low cirrus coverages ($f \lesssim$
 350 0.45), and colder for relatively high coverages. Since no
 351 change other than the cirrus coverage in the tropical column
 352 is made, all change in temperature with cloud coverage in
 353 the extratropical column shown in Figure 1b is due to the
 354 transport from the tropical column. Figure 1d shows the
 355 global mean surface temperature (calculated as simply the
 356 average between the surface temperature in the two col-

umns). We see that for constant atmospheric composition 357
 (that is following a line of constant $f = 0.16$ in Figure 1d) the 358
 global mean surface temperature in our two-column model 359
 remains below freezing up until $S = 0.86 S_0$ giving some- 360
 what warmer temperatures than with previous 1-D radiative- 361
 convective simulations ($\sim 265 \text{ K}$ at $S = 0.8 S_0$ compared to 362
 $\sim 262 \text{ K}$ for the same insolation as in work by *Haqq-Misra* 363
et al. [2008]). We are confident that these differences are not 364
 due to the peculiarities of the radiative parameterization or 365
 to the convective adjustment since our own 1-D tropical 366
 simulations with no cloud cover can be used to recover a 367
 temperature of about 263 K for $S = 0.8 S_0$ similar to the ones 368
 reported for current atmospheric composition at $S = 0.8 S_0$ 369
 [Kasting and Catling, 2003; *Haqq-Misra et al.*, 2008]. 370

[20] The dashed curves in Figure 1d indicate that for 371
 some value of γ between $-10\%/K$ and $-20\%/K$, there is a 372
 solution of the paradox up to $S = 0.8 S_0$ or for a the range 373
 between 2.9 and 1.9 Ga. This solution would imply a total 374
 cirrus coverage for the tropics, and a tropical mean temper- 375
 ature of about 285 K . A smaller rate of change of about 376
 $-7\%/K$ however, can sustain global mean temperatures of 377
 only $\sim 261 \text{ K}$ for $S = 0.72 S_0$, although tropical mean 378
 surface temperatures in this case would be just above 379
 freezing, suggesting that even this moderate rate of change 380
 in cloud coverage could explain ice-free conditions for large 381
 regions of Earth. 382

3.3. Thin Cirrus and Increased Greenhouse Gases 383

[21] CO_2 alone can provide enough greenhouse effect to 384
 overcome the paradox. However, geological evidence seems 385
 to point to less CO_2 present in the atmosphere than would 386
 be required. For instance, *Rye et al.* [1995] argue on the 387
 basis of the absence of siderite that CO_2 concentrations 388
 higher than about 10 times the present atmospheric level 389
 (10 PAL) at 273 K are unlikely at about 2.8 Ga ($S \sim 0.81 S_0$). 390
 This limit is temperature-dependent and goes up to about 391
 50 PAL at temperatures above 300 K . *Kasting* [1993] quotes 392
 levels of CO_2 that are several times higher than the paleosol 393
 limit ($\sim 50 \text{ PAL}$ for reaching $T_s \sim 273 \text{ K}$ for $S = 0.8 S_0$). The 394
 discrepancy between required and estimated CO_2 concen- 395
 trations is also found in other geological and theoretical 396
 evidence [see, e.g., *Rollinson*, 2007, and references therein]. 397
 CH_4 , with a much longer lifetime in an anoxic atmosphere 398
 than in the present atmosphere, could provide an additional 399
 greenhouse effect. However, recent calculations by *Haqq-* 400
Misra et al. [2008] show that the required concentrations of 401
 CH_4 are larger than previously believed. Also the CH_4 402
 greenhouse effect is limited by the formation of a reflective 403
 organic haze when CH_4/CO_2 is higher than ~ 1 . 404

[22] In this section, we will show calculations with a thin 405
 cirrus cloud feedback as the one previously described, 406
 operating at the same time as an atmosphere with larger 407
 CO_2 concentrations. We perform the same runs as in the 408
 control case for three different CO_2 concentrations for $S =$ 409
 $0.8 S_0$. The longwave parameterization by *Chou et al.* 410
 [2002] is deemed appropriate even for concentrations of 411
 about 100 times present atmospheric levels of CO_2 . 412

[23] Figure 2 shows the surface temperature for three 413
 different CO_2 concentrations at $S = 0.8 S_0$. We see that for 414
 the current climate value of $f = 0.16$ (vertical dashed grey 415
 line) and for the present value of CO_2 (1 PAL), the surface 416
 temperature is about 266 K . For a constant cloud coverage 417

t1.1 **Table 1.** Value of the Cloud Microphysical and Radiative Properties for the Sensitivity Runs^a

t1.2	cwc (10^{-4} g/g)	IWP (g/m ²)	τ	r_e (μ m)	LW (W/m ²)	SW (W/m ²)	NET (W/m ²)
t1.3	7	46	1.3	59	120	-70	50
t1.4	3.5	23	0.73	52	70	-35	35
t1.5	28	185	4	75	140	-130	10

^aAbbreviations: cwc, cloud water content; τ , visible optical depth; and LW, SW, and NET, the cloud radiative forcing in the longwave, shortwave, and net, respectively. For all runs the thickness of the cloud is fixed at ~ 200 m, and the cloud is located at 200 hPa.

t1.6

418 the amount of CO₂ required for mean global temperatures to
 419 rise above 273 is about 20 PAL CO₂. We recover here the
 420 well-known result that the paradox cannot be solved solely
 421 on the basis of a higher concentration of CO₂, without
 422 getting a result inconsistent with the paleosol data. If we
 423 focus on values of CO₂ allowed by the paleosol constraints,
 424 a solution to the paradox can be found with relatively small
 425 values for the cloud feedback magnitude. For instance, for
 426 1 PAL CO₂, the tropical coverage required to solve the
 427 paradox is about 1. For the case in which CO₂ \sim 10 PAL,
 428 the paradox can be solved with a tropical coverage of only
 429 0.35 and the magnitude of the cloud rate of change required
 430 for providing these cloud coverage is $\gamma \sim -5\%/K$. This
 431 solution is just barely consistent with the paleosol constraint
 432 and of course stronger values of the cloud feedback could
 433 solve the paradox for lower levels of CO₂. We stress that
 434 both consistency with the paleosol data and global mean
 435 temperatures above freezing can be achieved (at least for
 436 this particular value of solar insolation) invoking only a
 437 small magnitude of the cloud rate of change. We also note
 438 that while cirrus coverage is less than full, the effect of
 439 further increasing cirrus coverage in the mean temperature
 440 is mostly linear with cloud coverage as opposed to the effect
 441 of the increase in CO₂ (or other greenhouse gases) in the
 442 mean temperature that are only logarithmic.

3.4. Sensitivity to Cloud Water Content

443

[24] Our results so far, have been obtained with a single
 444 cloud with optical depth 1.3. We explore the sensitivity to
 445 changes in the cloud water content of the cloud. Table 1
 446 summarizes the cloud properties of the different clouds. The
 447 cloud radiative effects were calculated with the runs
 448 corresponding to $f = 0.2$. The clouds with either much
 449 larger or much smaller cloud water content than the control
 450 case produce smaller net radiative effects. Even though
 451 there is a net positive cloud radiative effect for the cwc
 452 (cloud water content) = 28×10^{-4} run, the cloud radiative
 453 effect becomes negative for higher cloud fractions and
 454 temperatures decrease with cloud coverage (Figure 3b).
 455 For the thinner cloud case, the net radiative effect is smaller
 456 but positive and very similar to the control case (Figure 3a).
 457 This “optimal” net radiative for the control case coincides
 458 with the ordering provided by *Choi and Ho* [2006] with
 459 respect to shortwave optical depth; smaller positive radiative
 460 effect for thinner clouds and smaller and even negative
 461 radiative effects for thicker clouds.
 462

3.5. Sensitivity to the Fixed Height Assumption

464

[25] We have also tested the possibility that the results are
 465 sensitive to the assumption of a fixed height or fixed
 466 pressure level cloud. An alternative to specifying the cloud
 467 at a constant pressure level is the fixed anvil temperature
 468 proposed by *Hartmann and Larson* [2002]. They propose
 469 that the level at which radiative cooling decreases substan-
 470 tially is controlled by the distribution of water vapor. At the
 471 same time, the total amount of water vapor is a strong
 472 function of temperature as a consequence of the Clausius-
 473 Clapeyron relation. Therefore, radiative cooling rates in the
 474 troposphere are a strong function temperature (as long as
 475 water vapor is the main driver of the radiative cooling). The
 476 divergence of the radiative cooling would then occur at
 477 about the same temperature no matter the surface temper-
 478 ature of the climate considered. Since convective heating
 479 balances radiative cooling in the tropical free troposphere,
 480

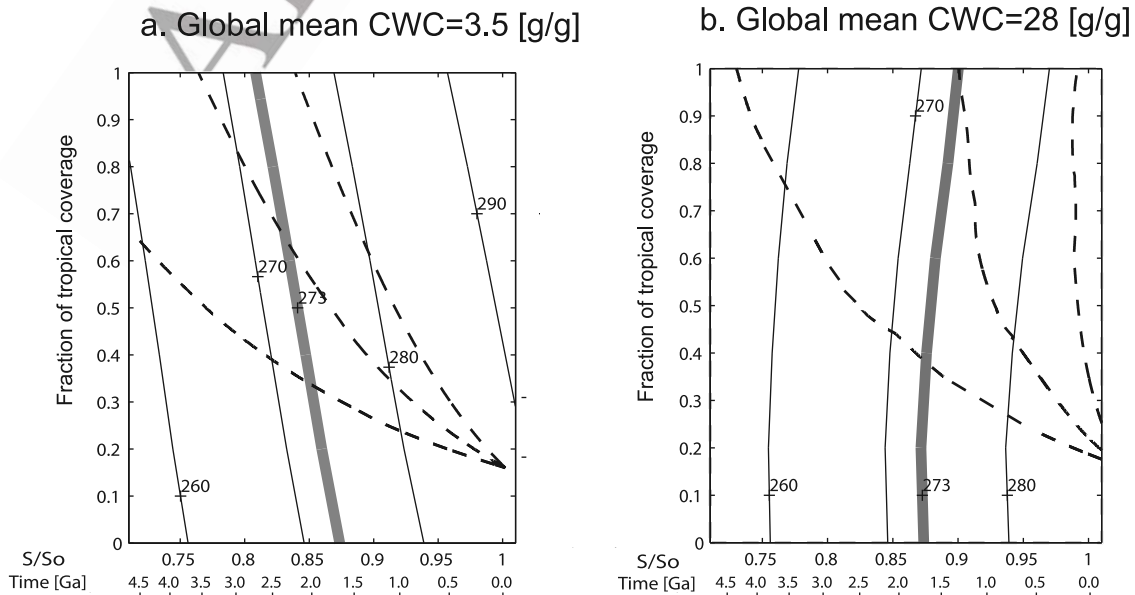


Figure 3. Same as Figure 1d but for clouds with different cloud water content: (a) 3.5 g/g and (b) 28 g/g.

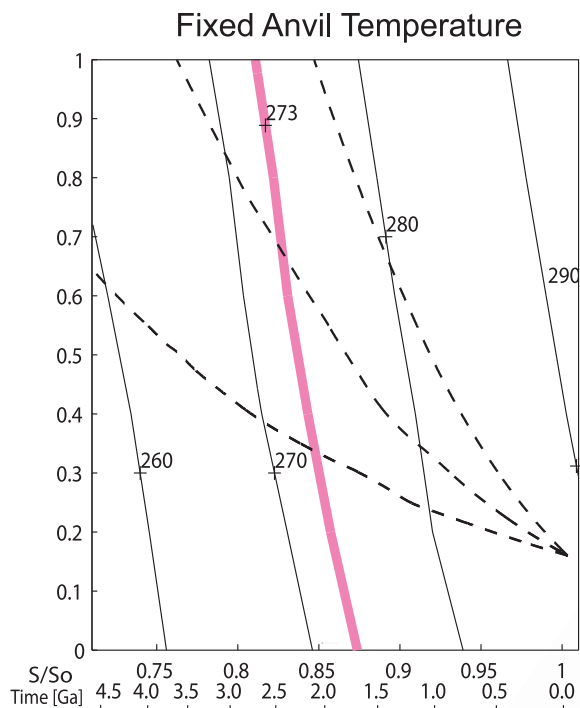


Figure 4. Same as Figure 1d but for a fixed temperature anvil cloud at the 220 K level.

481 the level at which convection detrains would be strongly
 482 constrained to be near a fixed temperature. In Figure 4 we
 483 show the results for the global mean surface temperature for
 484 the two-column model in the case in which the cloud is
 485 located at the 220 K level (this is done iteratively at each
 486 time step in the tropical column). The results show that the
 487 magnitude of the cloud effect is only modestly reduced. For
 488 instance for $S = 0.81 S_0$, the tropical coverage required for
 489 global mean temperatures to be above 273 K in the control
 case is $f \gtrsim 0.87$. For the fixed anvil temperature case $f \sim 1$.

491 3.6. Sensitivity to Water Vapor Feedback

492 [26] So far we have followed the customary assumption
 493 of a constant relative humidity profile. In the context of our
 494 1-D single column tropical model, the assumption of strict
 495 relative humidity invariance gives a water vapor feedback
 496 factor, $\beta \sim 0.4$. Recent studies suggest that the strong
 497 positive water vapor feedback implied by the invariance
 498 of relative humidity may be within reasonable agreement
 499 with satellite observations [Dessler *et al.*, 2008], even
 500 though the vertical profile of relative humidity is not strictly
 501 conserved [see also Sun and Held, 1996]. Renno *et al.*
 502 [1994], for instance, showed in the context of a radiative-
 503 convective equilibrium model with an explicit hydrological
 504 cycle, that changes in the microphysical parameters that
 505 control the conversion of water to precipitation and vapor
 506 could produce very different equilibrium climates, with
 507 different vertical distributions of relative humidity. Since
 508 we do not have an explicit parameterization for water vapor
 509 in our model, we specify changes in relative humidity with
 510 surface temperature to explore the sensitivity of the results
 511 to the water vapor feedback strength.

[27] We vary the relative humidity in the model from the 512
 original relative humidity profile according to 513

$$\text{RH}(500 \text{ hPa}) = \alpha \times (T_s - 288) + \text{RH}_0(500 \text{ hPa}), \quad (4)$$

where RH_0 is the original relative humidity (based on the 514
 Manabe and Wetherald [1967] profile). Between 200 hPa 516
 and 800 hPa, the humidity profile is interpolated from the 517
 original profile to the new value at 500 hPa using a cubic 518
 spline. Since we have specified the change in the feedback 519
 in terms of a change in relative humidity, the magnitude of 520
 the feedback will have a dependence on temperature. We 521
 use the model output to calculate the magnitude of the water 522
 vapor feedback for each case. Figure 5 shows the 523
 temperature dependence of the feedback factor for three 524
 different values of $\alpha = -0.015, 0, +0.015$. The feedback 525
 factor decreases with temperature for all cases. For the 526
 imposed changes in relative humidity, the spread of the 527
 water vapor feedback tends to decrease with temperature. 528
 This is already an indication that uncertainties in the water 529
 vapor feedback factor for current climate will be less 530
 consequential in determining the temperature for lower 531
 global mean surface temperatures. 532

[28] Figure 6 shows the mean surface temperature for 533
 two-column model as a function of the cloud fraction for 534
 $S = 0.8 S_0$. Global mean temperatures ~ 273 K, are found at 535
 $f \sim 1$. Changing α from $-0.015/\text{K}$ to $0.015/\text{K}$ has little 536
 effect on the total cirrus cloud cover needed for temper- 537
 atures above freezing. Figure 6 also hints to the fact that 538
 changes in water vapor feedback are more efficient for 539
 relatively low cloud coverage, since changes in water vapor 540
 in the free troposphere are buffered by the presence of the 541
 cloud above (notice the shaded regions in Figure 6 showing 542
 the reduced range of variation in f required for a given 543
 temperature for low coverage). The two effects, namely the 544
 decrease in strength of the feedback with temperature and 545

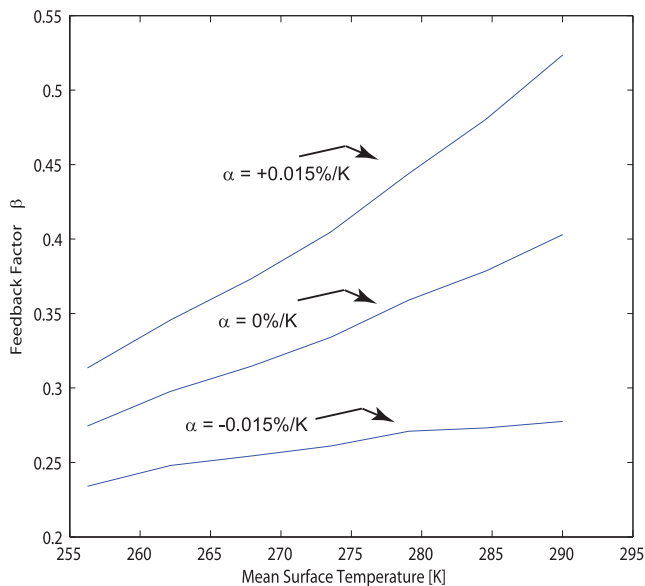


Figure 5. Water vapor feedback factor β as a function of temperature for three different values of the strength of the relative humidity change in equation (4) ($\alpha = -0.015, 0$, and 0.015).

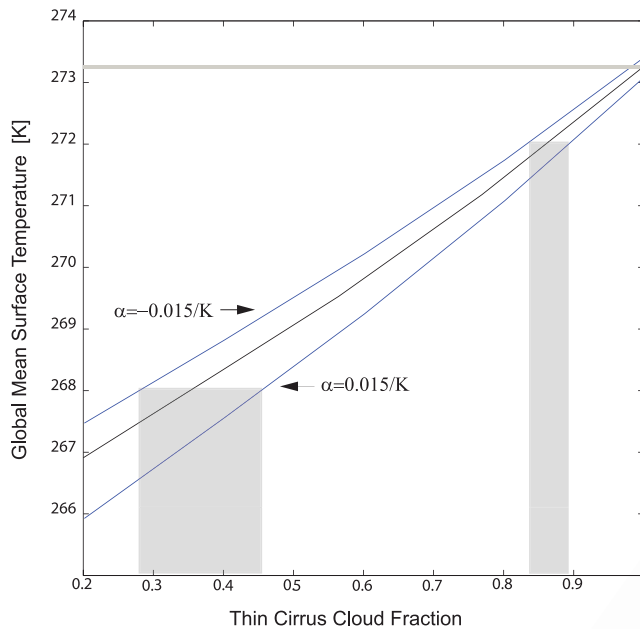


Figure 6. Sensitivity of the results for $S = 0.8S_0$ to the water vapor feedback strength. The two shaded regions show the value of the cloud coverage required to obtain a given global mean temperature (in this case 268 and 272 K).

546 the decrease in strength of the feedback for large cirrus
547 coverage, suggest that the range of the solution has a low
548 sensitivity to the strength of the water vapor feedback in the
549 context of the present model.

550 3.7. Sensitivity to the Meridional Heat Flux

551 [29] We have so far assumed a linear diffusivity law for
552 the heat transport between the tropical and extratropical
553 column. An alternative to the simple linear diffusivity
554 would be to assume a constant temperature difference
555 between the two columns so as to crudely represent a
556 baroclinic adjustment over the different possible climates
557 considered [e.g., Stone, 1978]. This is accomplished in the
558 model by allowing the diffusivity coefficient to change
559 while keeping a constant target temperature difference
560 between the two columns (in this case 20 K). In Figure 7
561 we see the result of this modification. The situation in the
562 global mean is not very different from the constant diffusivity
563 depicted in Figure 1d, so that the main result does not
564 change appreciably; the mean global temperature can be
565 above freezing for luminosities ~ 0.81 and full tropical
566 cirrus coverage. However, since in the case of the fixed
567 temperature difference the tropics are colder than in the
568 control case (for instance, the mean tropical temperature is
569 282 K for $S = 0.81 S_0$ and $f = 1$ in the fixed meridional
570 temperature case and 285 K in the linear diffusivity case for
571 the same conditions) the values of γ required to accomplish
572 the needed full tropical cirrus coverage are therefore smaller
573 in the fixed meridional temperature case ($\gamma \sim -12\%/K$
574 compared to $\gamma \sim -15\%/K$ in the control case). By provid-
575 ing warmer extratropical temperatures, this alternative treat-
576 ment for the meridional heat flux would also delay the onset
577 of solutions unstable to an eventual ice-albedo feedback.
578 Besides the control case and the constant temperature case,

we have a third assumption about the meridional heat 579
transport. In the case of a single column tropics depicted 580
in Figure 1 the meridional heat transport is implicit (since 581
the incoming solar radiation is tuned to obtain current 582
tropical temperatures) and reduced by the same fraction as 583
the reduction in incoming solar radiation. In the single 584
column tropical cases the heat transport becomes less 585
effective as the climate cools (similar to the decrease in 586
transport efficiency predicted from maximum entropy con- 587
siderations [Gerard *et al.*, 1990]). This isolation of the 588
tropics from the extratropics also allows for a more effective 589
functioning of the tropical cirrus clouds in resisting the 590
changes in the solar constant and would provide a more 591
robust “partial” solution to the paradox, with relatively 592
warm oceans in the tropical regions of the planet. 593
594

4. Discussion 595

[30] We have presented simplified radiative-convective 596
equilibrium calculations to investigate the role of thin cirrus 597
clouds in providing a solution for the faint young Sun 598
paradox. In the context of our model, solutions do in fact 599
exist. Tropical thin cirrus clouds can either solve the 600
paradox in the sense of providing *global* mean temperatures 601
above freezing (after ~ 2.9 Ga) or in a weaker sense, less 602
than full tropical cirrus coverage can provide *tropical* mean 603
temperatures above freezing for all Earth’s existence (in the 604
context of this model). The solutions are characterized by a 605
colder tropical temperature and therefore by thin cirrus 606
clouds acting as a net negative feedback to the solar forcing. 607

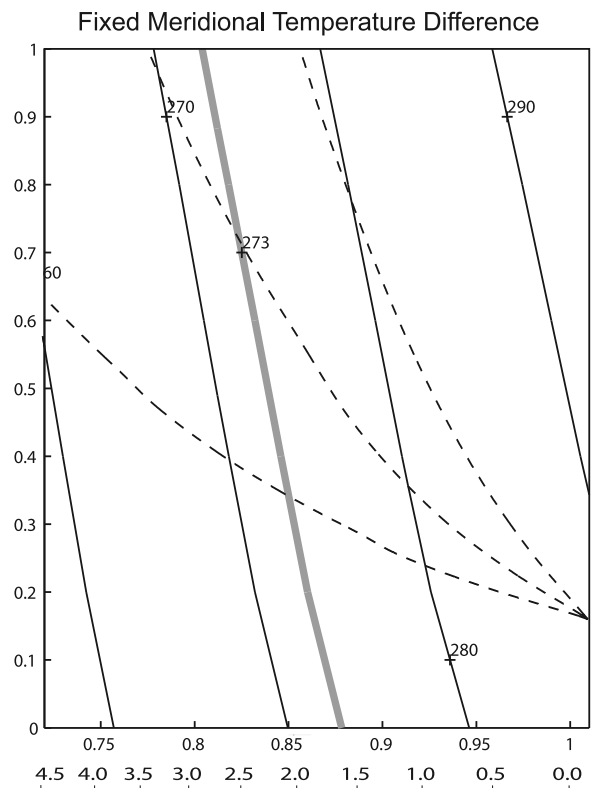


Figure 7. Same as Figure 1d but for a fixed difference in surface temperature between the tropical and the extra-tropical column.

608 [31] Given that thin cirrus clouds can indeed solve the
 609 paradox, we focus the discussion on the question of the
 610 plausibility of these solutions. There is the suggestion that a
 611 negative feedback such as the one required might in fact be
 612 operating in current climate [Lindzen *et al.*, 2001]. Accord-
 613 ing to this suggestion, called the iris hypothesis, an increase
 614 in sea surface temperature (through an increase in the
 615 specific humidity of the air that participates in convection)
 616 can make precipitation in convective clouds more efficient.
 617 In this way less condensate is rained out from deep
 618 convective clouds and therefore more condensate is avail-
 619 able to be detrained from the top of the cloud to form cirrus
 620 clouds. The iris hypothesis is controversial and it would be
 621 lengthy to discuss all the arguments here. Apparent confir-
 622 mation for the iris effect came from the analysis of the OLR
 623 trends over the last two decades, showing a strong increase
 624 in the OLR compared to a relatively smaller decrease in the
 625 shortwave reflectivity in the tropics [Wielicki *et al.*, 2002;
 626 Chen *et al.*, 2002]. Using a combination of data sets,
 627 Hatzidimitriou *et al.* [2004] traced the OLR increase mainly
 628 to a decrease in the upper level cloud coverage and a drying
 629 of the upper troposphere. As pointed out by Chou and
 630 Lindzen [2005] this large increase in OLR was also consis-
 631 tent with a much larger value in the relative change in cloud
 632 fraction with temperature than the original $-22\%/K$ found
 633 by Lindzen *et al.* [2001]. The OLR trends were recently
 634 revised down to only about a quarter of the original value
 635 [Wong *et al.*, 2006], although the OLR trend continues to be
 636 larger than the Planck response expected from an increase in
 637 the tropical mean temperature over the same period.
 638 Recently, Lindzen and Choi [2009] studied variations in
 639 the outgoing radiative fluxes with respect to changes in the
 640 average tropical temperature in intraseasonal scales. A total
 641 negative feedback was deduced from the outgoing long-
 642 wave response of the tropics. If a strong positive water
 643 vapor feedback is realistic [e.g., Dessler *et al.*, 2008], then
 644 the combined effect of water vapor feedback and lapse rate
 645 feedback must be more than compensated by a strong
 646 unknown process acting on modifying the longwave flux.
 647 This process cannot be distinguished from the bulk of the
 648 longwave response in the analysis by Lindzen and Choi
 649 [2009], but it most likely resides in the combined behavior
 650 of clouds and water vapor in the tropics. This leaves open
 651 the possibility that a negative feedback such as the iris is
 652 operating in the present climate.

653 [32] We have assumed so far that the magnitude of the
 654 cloud changes with respect to temperature is absolute, that
 655 is, they already contain any possible dependence on changes
 656 in convective activity that will arise as the incoming
 657 radiation at the surface decreases. Theoretical arguments
 658 and model simulations both indicate that changes in precip-
 659 itation with global mean temperature are relatively small
 660 ($\sim 2\text{--}4\%/K$ [Held and Soden, 2006; O’Gorman and
 661 Schneider, 2008]). A correction to account for the reduction
 662 of precipitation or convective activity will indeed be
 663 required. One can diagnose from the surface budget, the
 664 total convective heating in the model, which, in the tropics
 665 has to be equal to the precipitation. The changes in
 666 precipitation in the model depend on the magnitude of the
 667 feedback itself, given that a stronger feedback would reduce
 668 the net incoming solar radiation at the surface more rapidly
 669 than in the case of a weaker feedback. This is illustrated in

Figure 8 which shows the increase in precipitation with 670
 temperature for three different values of the absolute cloud 671
 change γ . One can write $\gamma = \gamma' + \frac{1}{P} \frac{\partial P}{\partial T}$, so that the relative 672
 changes in cloud fraction γ' , have to be higher in magnitude 673
 than the magnitude of the change γ required to compensate 674
 for the decrease of precipitation in a colder climate. Fitting 675
 exponential functions to the model-diagnosed precipitation 676
 one finds that the quantity $\frac{1}{P} \frac{\partial P}{\partial T}$ goes from about $3\%/K$ to 677
 $7\%/K$. 678

[33] Regarding observed value of γ' , different data sets 679
 and analyses point to values between $-2\%/K$ to $-22\%/K$ 680
 for current climate (see R. Rondanelli and R. S. Lindzen, 681
 Comments on “Variations of tropical upper tropospheric 682
 clouds with sea surface temperature and implications for 683
 radiative effects,” submitted to *Journal of Geophysical* 684
Research, 2010) for a discussion of some of the methodo- 685
 logical issues involved). These empirically derived rates of 686
 change γ' , usually refer to some observable that is a proxy 687
 for the thin cirrus clouds rather than the thin cirrus clouds 688
 themselves. Nevertheless, the magnitude of these changes is 689
 consistent with what is required to solve the paradox (for 690
 instance from Figures 1c and 1d, the tropical temperature 691
 for $S = 0.8 S_0$ and $f = 1$ is about 285 K which gives a rate of 692
 change of $\gamma \sim -15\%/K$, $\gamma' \sim -20\%/K$). 693

[34] One can ask what happens in the situation in which 694
 the tropical atmosphere is already completely covered by 695
 cirrus clouds and temperatures continue to decrease. One 696
 could expect that if the cloud feedback still operates beyond 697
 full coverage, an increase in the cloud water content or in 698
 the thickness of the cirrus clouds would ensue. The cloud 699
 feedback can only operate until the cloud is thick enough 700
 ($\tau \sim 10$) that surface cooling instead of heating is obtained 701
 (as in Figure 3b). At the same time, if the cloud cover is 702
 thick enough to reflect most of the incoming solar radiation, 703
 convection (and therefore the source of the cloud) will shut 704
 off. Microphysical effects such as an enhanced precipitation 705
 from the cirrus cloud might prevent this from happening. 706
 However, without a mechanistic model one cannot go 707
 beyond speculation on this point. We only note here that 708
 the mechanism such as the one described will have a limit 709
 for low temperatures. The availability of water for sustain- 710
 ing a total cirrus coverage does not pose a problem. Even 711
 with a weaker hydrological cycle as expected in a colder 712
 climate (rainfall rate estimated in ~ 2 mm/d for a surface 713
 temperature of ~ 270 K [O’Gorman and Schneider, 2008]) 714
 and with a 44 g/m² cloud (with an accompanying water 715
 vapor layer of 400 g/m²) and assuming that a typical ice 716
 particle dissipates over a day, the detrainment flux required 717
 to sustain such a cloud is only about $\sim 2\%$ of the precipi- 718
 tation rate. 719

[35] Although the literature about the paradox usually 720
 focuses on greenhouse gas solutions [Kasting and Catling, 721
 2003; Shaw, 2008], solutions based on cloud feedbacks 722
 have been put forth in the past. Based on the model 723
 developed by Wang *et al.* [1981] in which cloud cover is 724
 considered proportional to the convective heating (or total 725
 precipitation), Rossow *et al.* [1982] [see also McGuffie and 726
 Henderson-Sellers, 2005, section 4.6.1] proposed a solution 727
 to the paradox based on the negative feedback resulting 728
 from a decrease in planetary albedo and a decrease in the 729
 cloud water content (and therefore in the visible optical 730
 depth) of clouds in a colder climate. Our solution on the 731

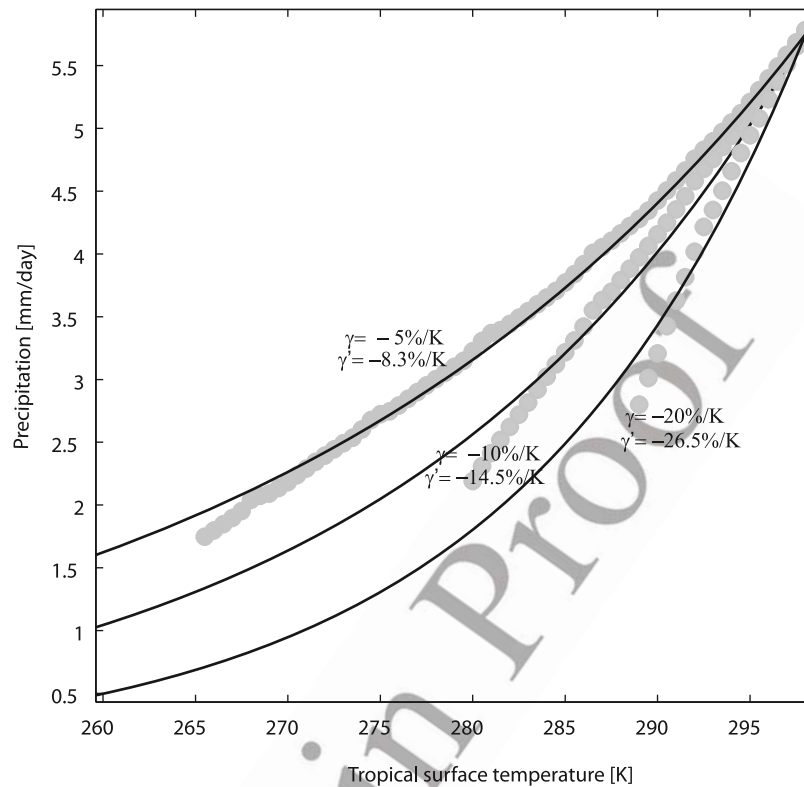


Figure 8. Changes in precipitation diagnosed from the surface balance in the tropical column of the model. The gray dots show the precipitation diagnosed from the model for three values of the magnitude of the feedback $\gamma = 5, 10,$ and $20\%/K$. The black lines are exponential fits to the precipitation curves from which a value of γ' was deduced.

732 other hand leaves the albedo almost unchanged as it mostly
 733 depends on the longwave radiative effect of upper level thin
 734 cirrus clouds. The solution by *Rossow et al.* [1982] and our
 735 solution are not mutually exclusive. Several cloud feed-
 736 backs other than the one resulting from the change in thin
 737 cirrus are possible in reality and have been muted in the
 738 present model (for instance area coverage and composition
 739 of stratocumulus clouds in the subtropics). Despite progress
 740 since the time of the writing of the study by *Rossow et al.*
 741 [1982], clouds continue to be “the major source of uncer-
 742 tainty” in climate models [e.g., *Schwartz, 2008*]. As in
 743 previous studies dealing with clouds and the faint young
 744 Sun problem (*Cogley and Henderson-Sellers* [1984] pro-
 745 vide references to previous work on this issue) (see also the
 746 mechanism proposed by *Shaviv* [2003]), we conclude that a
 747 negative cloud feedback can indeed solve the paradox if the
 748 Archean climate was somewhat colder than present. (How
 749 much colder will also depend on the strength of the
 750 feedback.) We have followed the customary assumptions
 751 of neglecting the ice-albedo feedback, fixing the relative
 752 humidity and muting the effect of clouds to a large extent,
 753 we have also assumed a very simplified treatment for the
 754 heat transport between tropics and extratropics. None of
 755 these assumptions is entirely satisfactory. Given the simpli-
 756 fied nature of this radiative-convective model, our study is
 757 only exploratory.

758 [36] Solving the paradox down to a luminosity of $S =$
 759 $0.8 S_0$, requires a climate with an equilibrium sensitivity
 760 parameter to solar forcing $\lambda = \Delta T_s / \Delta S$ of about 0.29 K/

(W m^{-2}) . This sensitivity value is certainly smaller than 761
 any of the sensitivities to CO_2 forcing in current GCMs 762
 [*Intergovernmental Panel on Climate Change, 2007*], but it 763
 is within the lower range of estimates made from observa- 764
 tions [e.g., *Schwartz, 2008*]. One finds values of $\lambda \sim 0.4 \text{ K/}$ 765
 (W m^{-2}) for the 1-D radiative-convective models without 766
 clouds (using for instance the results by *Kasting* [1987]); we 767
 also found a nearly identical value for λ in our two-column 768
 radiative convective model with no cloud feedback. As 769
 shown in section 3.3, small changes in the rate of change 770
 of cloud coverage can reduce the amount of greenhouse 771
 gases needed to reach consistency with the geological 772
 evidence. These clouds changes are associated with small 773
 changes in the model climate sensitivity (a $-5\%/K$ rate of 774
 change in the thin cirrus coverage is equivalent to a 775
 sensitivity $\lambda \sim 0.37 \text{ K}/(\text{W m}^{-2})$) in the present model). 776

5. Concluding Remarks

777

[37] Using simple radiative-convective simulations we 778
 have tested the idea that a coverage of tropical cirrus clouds 779
 much larger than present could resolve the faint young Sun 780
 paradox. We have found that relatively modest cloud 781
 changes can indeed provide sufficient cirrus coverage for 782
 the mean global temperature to be above freezing for $S \gtrsim$ 783
 $0.8 S_0$ and for the mean tropical temperature to be above 784
 freezing for $S \gtrsim 0.7 S_0$ without additional greenhouse gases. 785
 The model cloud is specified to have similar cloud radiative 786
 effect as reported in current climate observations. We tested 787

788 the sensitivity of the results to cloud water content, to the
789 assumption of a constant pressure level of detrainment and
790 to a range for the strength of the water vapor feedback. We
791 also looked at two different treatments for the meridional
792 heat transport. We find small sensitivities to all these factors
793 in the present model. Although we describe a very specific
794 cloud negative feedback, our results can be understood in a
795 more general perspective with respect to the faint young
796 Sun paradox; a moderate negative climate feedback can
797 indeed resolve the paradox without resorting to large
798 changes in the greenhouse gas content of the Archean
799 atmosphere.

800 [38] **Acknowledgments.** We thank M.D. Chou for providing us with
801 the radiative code used in this study. Comments by Yong-Sang Choi and
802 Jacob Haqq-Misra on earlier versions of the manuscript are appreciated. We
803 also appreciate a thoughtful review by Dorian Abbott and comments from
804 two anonymous reviewers that helped to improve the manuscript.

805 References

- 806 Catling, D., and J. Kasting (2007), Planetary atmospheres and life, in
807 *Planets and Life: The Emerging Science of Astrobiology*, pp. 91–116,
808 Cambridge Univ. Press, Cambridge, U. K.
- 809 Chen, J., B. Carlson, and A. Del Genio (2002), Evidence for strengthening
810 of the tropical general circulation in the 1990s, *Science*, 295(5556), 838–
811 841.
- 812 Choi, Y.-S., and C.-H. Ho (2006), Radiative effect of cirrus with different
813 optical properties over the tropics in MODIS and CERES observations,
814 *Geophys. Res. Lett.*, 33, L21811, doi:10.1029/2006GL027403.
- 815 Chou, M., and R. Lindzen (2005), Comments on “Examination of the
816 decadal tropical mean ERBS nonscanner radiation data for the iris
817 hypothesis,” *J. Clim.*, 18(12), 2123–2127.
- 818 Chou, M., and M. Suarez (2002), A Solar Radiation parameterization for
819 atmospheric studies, *NASA Tech. Memo, TM-1999-10460*, vol. 15, 52 pp.
- 820 Chou, M., K. Lee, S. Tsay, and Q. Fu (1999), Parameterization for cloud
821 longwave scattering for use in atmospheric models, *J. Clim.*, 12(1), 159–
822 169.
- 823 Chou, M., K. Lee, and P. Yang (2002), Parameterization of shortwave cloud
824 optical properties for a mixture of ice particle habits for use in atmo-
825 spheric models, *J. Geophys. Res.*, 107(D21), 4600, doi:10.1029/
826 2002JD002061.
- 827 Chou, M. D., M. J. Suarez, X.-Z. Liang, and M. M.-H. Yan (2003), A
828 Thermal Infrared Radiation Parameterization for Atmospheric studies,
829 *NASA Tech. Memo, TM-2001-104606*, vol. 19, 55pp.
- 830 Cogley, J., and A. Henderson-Sellers (1984), The origin and earliest state of
831 the Earth’s hydrosphere, *Rev. Geophys.*, 22(2), 131–175.
- 832 Dessler, A. E., Z. Zhang, and P. Yang (2008), Water-vapor climate feedback
833 inferred from climate fluctuations, 2003–2008, *Geophys. Res. Lett.*, 35,
834 L20704, doi:10.1029/2008GL035333.
- 835 Emanuel, K. A. (2007), Quasi-equilibrium dynamics of the tropical atmo-
836 sphere, in *The Global Circulation of the Atmosphere*, pp. 186–218,
837 Princeton Univ. Press, Princeton, N. J.
- 838 Endal, A., and K. Schatten (1982), The faint young Sun-climate paradox:
839 Continental influences, *J. Geophys. Res.*, 87, 7295–7302.
- 840 Gerard, J., D. Delcourt, and L. Francois (1990), The maximum entropy
841 production principle in climate models: Application to the faint young
842 Sun paradox, *Q. J. R. Meteorol. Soc.*, 116, 1123–1132, doi:10.1256/
843 smsj.49505.
- 844 Gough, D. (1981), Solar interior structure and luminosity variations, *Sol.*
845 *Phys.*, 74(1), 21–34.
- 846 Haqq-Misra, J. D., S. D. Domagal-Goldman, P. J. Kasting, and J. F. Kasting
847 (2008), A revised, hazy methane greenhouse for the Archean Earth,
848 *Astrobiology*, 8(6), 1127–1137, doi:10.1089/ast.2007.0197.
- 849 Hart, M. (1978), The evolution of the atmosphere of the Earth, *Icarus*, 33,
850 23–39.
- 851 Hartmann, D., and K. Larson (2002), An important constraint on tropical
852 cloud–climate feedback, *Geophys. Res. Lett.*, 29(20), 1951, doi:10.1029/
853 2002GL015835.
- 854 Hatzidimitriou, D., I. Vardavas, K. Pavlakis, N. Hatzianastassiou,
855 C. Matsoukas, and E. Drakakis (2004), On the decadal increase in the
856 tropical mean outgoing longwave radiation for the period 1984–2000,
857 *Atmos. Chem. Phys.*, 4, 1419–1425.
- 858 Held, I., and B. Soden (2006), Robust responses of the hydrological cycle
859 to global warming, *J. Clim.*, 19(21), 5686–5699.
- Henderson-Sellers, A., and J. G. Cogley (1982), The Earth’s early hydro- 860
sphere, *Nature*, 298, 832–835. 861
- Intergovernmental Panel on Climate Change (2007), *Climate Change 2007:* 862
The Physical Science Basis, edited by S. Solomon et al., Cambridge Univ. 863
Press, Cambridge, U. K. 864
- Kasting, J. (1987), Theoretical constraints on oxygen and carbon dioxide 865
concentrations in the Precambrian atmosphere, *Precambrian Res.*, 34(3–4), 866
205–229. 867
- Kasting, J. (1993), Earth’s early atmosphere, *Science*, 259(5097), 920–926. 868
- Kasting, J., and D. Catling (2003), Evolution of a habitable planet, *Annu.* 869
Rev. Astron. Astrophys., 41, 429–463. 870
- Kasting, J., O. Toon, and J. Pollack (1988), How climate evolved on the 871
terrestrial planets, *Sci. Am.*, 258(2), 90–97. 872
- Kuhn, W., and S. Atreya (1979), Ammonia photolysis and the greenhouse 873
effect in the primordial atmosphere of the Earth, *Icarus*, 37, 207–213. 874
- Lindzen, R. S., and Y.-S. Choi (2009), On the determination of climate 875
feedbacks from ERBE data, *Geophys. Res. Lett.*, 36, L16705,
doi:10.1029/2009GL039628. 876
- Lindzen, R., and B. Farrell (1980), The role of polar regions in global 877
climate, and a new parameterization of global heat transport, *Mon. Weather* 878
Rev., 108(12), 2064–2079. 879
- Lindzen, R. S., M.-D. Chou, and A. Y. Hou (2001), Does the Earth have an 880
adaptive infrared iris?, *Bull. Am. Meteorol. Soc.*, 82(3), 417–432. 881
- Liou, K. (2005), Cirrus clouds and climate, in *Yearbook of Science and* 882
Technology, pp. 51–53, McGraw-Hill, New York. 883
- Liou, K., and K. Gebhart (1982), Numerical experiments on the thermal 884
equilibrium temperature in cirrus cloudy atmospheres, *J. Meteorol. Soc.* 885
Jpn., 60, 570–582. 886
- Lovelock, J., and M. Whitfield (1982), Life span of the biosphere, *Nature*, 887
296, 561–563. 888
- Mace, G., M. Deng, B. Soden, and E. Zipser (2006), Association of tropical 889
cirrus in the 10–15-km layer with deep convective sources: An observa- 890
tional study combining millimeter radar data and satellite-derived trajec- 891
tories, *J. Atmos. Sci.*, 63(2), 480–503. 892
- Manabe, S., and R. Strickler (1964), Thermal equilibrium of the atmosphere 893
with a convective adjustment, *J. Atmos. Sci.*, 21(4), 361–385. 894
- Manabe, S., and R. Wetherald (1967), Thermal equilibrium of the atmo- 895
sphere with a given distribution of relative humidity, *J. Atmos. Sci.*, 24(3), 896
241–259. 897
- McFarquhar, G. (2001), Comments on ‘Parametrization of effective sizes of 898
cirrus-cloud particles and its verification against observations’ by Zhian 899
Sun and Lawrie Rikus (October B, 1999, 125, 3037–3055), *Q. J. R.* 900
Meteorol. Soc., 127, 261–266. 901
- McGuffie, K., and A. Henderson-Sellers (2005), *A Climate Modelling* 902
Primer, John Wiley, Hoboken, N. J. 903
- Minton, D., and R. Malhotra (2007), Assessing the massive young Sun 904
hypothesis to solve the warm young Earth puzzle, *Astrophys. J.*, 905
660(2), 1700–1706. 906
- Newman, M., and R. Rood (1977), Implications of solar evolution for the 907
Earth’s early atmosphere, *Science*, 198(4321), 1035–1037. 908
- O’Gorman, P., and T. Schneider (2008), The hydrological cycle over a wide 909
range of climates simulated with an idealized GCM, *J. Clim.*, 22(21), 910
5676–5685, doi:10.1175/2009JCLI2701.1. 911
- Owen, T., R. Cess, and V. Ramanathan (1979), Enhanced CO₂ greenhouse 912
to compensate for reduced solar luminosity on early Earth, *Nature*, 277, 913
640–642. 914
- Paltridge, G. (1978), The steady-state format of global climate, *Q. J. R.* 915
Meteorol. Soc., 104, 927–945. 916
- Pavlov, A., J. Kasting, L. Brown, K. Rages, and R. Freedman (2000), 917
Greenhouse warming by CH₄ in the atmosphere of early Earth, *J. Geo-* 918
phys. Res., 105, 11,981–11,990. 919
- Pavlov, A., M. Hurtgen, J. Kasting, and M. Arthur (2003), Methane-rich 920
Proterozoic atmosphere?, *Geology*, 31(1), 87–90. 921
- Pierrehumbert, R. T. (2010), *Principles of Planetary Climate*, Cambridge 922
Univ. Press, Cambridge, U. K. 923
- Pinti, D. (2005), The origin and evolution of the oceans, in *Lectures in* 924
Astrobiology, vol. 1, edited by M. Gargaud et al., pp. 83–111, Springer, 925
New York. 926
- Renno, N., K. Emanuel, and P. Stone (1994), Radiative-convective model 927
with an explicit hydrologic cycle: 1. Formulation and sensitivity to model 928
parameters, *J. Geophys. Res.*, 99, 14,429–14,442, doi:10.1029/
94JD00020. 929
- Rollinson, H. (2007), *Early Earth Systems: A Geochemical Approach*, 930
Blackwell, Malden, Mass. 931
- Rossow, W., A. Henderson-Sellers, and S. Weinreich (1982), Cloud feed- 932
back: A stabilizing effect for the early Earth?, *Science*, 217(4566), 1245– 933
1247. 934
- Rye, R., P. Kuo, and H. Holland (1995), Atmospheric carbon dioxide con- 935
centrations before 2.2 billion years ago, *Nature*, 378, 603–605. 936

- 939 Sackmann, I., and A. Boothroyd (2003), Our Sun: V. A bright young Sun
940 consistent with helioseismology and warm temperatures on ancient Earth
941 and Mars, *Astrophys. J.*, 583(2), 1024–1039.
- 942 Sagan, C., and G. Mullen (1972), Earth and Mars: Evolution of atmo-
943 spheres and surface temperatures, *Science*, 177(4043), 52–56.
- 944 Sassen, K., Z. Wang, and D. Liu (2008), Global distribution of cirrus clouds
945 from CloudSat/Cloud-Aerosol Lidar and Infrared Pathfinder Satellite
946 Observations (CALIPSO) measurements, *J. Geophys. Res.*, 113,
947 D00A12, doi:10.1029/2008JD009972.
- 948 Schwartz, S. (2008), Uncertainty in climate sensitivity: Causes, conse-
949 quences, challenges, *Energy Environ. Sci.*, 1(4), 430–453.
- 950 Schwartzman, D., and T. Volk (1989), Biotic enhancement of weathering
951 and the habitability of Earth, *Nature*, 340, 457–460.
- 952 Schwartzman, D., and T. Volk (2004), Does life drive disequilibrium in the
953 biosphere?, in *Scientists Debate Gaia: The Next Century*, edited by S. H.
954 Schneider et al., pp. 129–135, MIT Press, Cambridge, Mass.
- 955 Schwarzschild, M. (1958), *Structure and Evolution of the Stars*, Princeton
956 Univ. Press, Princeton, N. J.
- 957 Shaviv, N. (2003), Toward a solution to the early faint Sun paradox: A
958 lower cosmic ray flux from a stronger solar wind, *J. Geophys. Res.*,
959 108(A12), 1437, doi:10.1029/2003JA009997.
- 960 Shaw, G. H. (2008), Earth's atmosphere—Hadean to early Proterozoic,
961 *Chem. Erde Geochem.*, 68(3), 235–264, doi:10.1016/j.chemer.2008.
962 05.001.
- 963 Stone, P. (1978), Baroclinic adjustment, *J. Atmos. Sci.*, 35(4), 561–571.
- 964 Sun, D., and I. Held (1996), A comparison of modeled and observed
965 relationships between interannual variations of water vapor and tempera-
966 ture, *J. Clim.*, 9(4), 665–675.
- Volk, T. (1987), Feedbacks between weathering and atmospheric CO₂ over 967
the last 100 million years, *Am. J. Sci.*, 287(8), 763–779. 968
- Walker, J., P. Hays, and J. Kasting (1981), A negative feedback mechanism 969
for the long-term stabilization of the Earth's surface temperature, *J. Geo-* 970
phys. Res., 86, 9776–9782. 971
- Wang, W., W. Rossow, M. Yao, and M. Wolfson (1981), Climate sensitivity 972
of a one-dimensional radiative-convective model with cloud feedback, 973
J. Atmos. Sci., 38(6), 1167–1178. 974
- Wielicki, B., et al. (2002), Evidence for large decadal variability in the 975
tropical mean radiative energy budget, *Science*, 295(5556), 841–844. 976
- Wilde, S., J. Valley, W. Peck, and C. Graham (2001), Evidence from detrital 977
zircons for the existence of continental crust and oceans on the Earth 978
4.4 Gyr ago, *Nature*, 409, 175–178. 979
- Wong, T., B. Wielicki, R. Lee III, G. Smith, K. Bush, and J. Willis (2006), 980
Reexamination of the observed decadal variability of the Earth Radiation 981
Budget using altitude-corrected ERBE/ERBS nonscanner WFOV data, 982
J. Clim., 19(16), 4028–4040. 983
- Zahnle, K., and N. H. Sleep (2002), Carbon dioxide cycling through the 984
mantle and implications for the climate of ancient Earth, *Geol. Soc. Spec.* 985
Publ., 199(1), 231–257, doi:10.1144/GSL.SP.2002.199.01.12. 986

R. S. Lindzen and R. Rondanelli, Department of Earth, Atmospheric and 987
Planetary Sciences, Massachusetts Institute of Technology, 54-1717, 989
77 Massachusetts Ave., Cambridge, MA 02139, USA. (rondane@mit.edu) 990